Nanoscale Res Lett (2008) 3:473–480
DOI 10.1007/s11671-008-9193-6

NANO REVIEW

Tube Formation in Nanoscale Materials

Chenglin Yan · Jun Liu · Fei Liu · Junshu Wu · Kun Gao · Dongfeng Xue

Received: 10 October 2008 / Accepted: 17 October 2008 / Published online: 4 November 2008

Abstract The formation of tubular nanostructures normally requires layered, anisotropic, or pseudo-layered crystal structures, while inorganic compounds typically do not possess such structures, inorganic nanotubes thus have been a hot topic in the past decade. In this article, we review recent research activities on nanotubes fabrication and focus on three novel synthetic strategies for generating nanotubes from inorganic materials that do not have a layered structure. Specifically, thermal oxidation method based on gas–solid reaction to porous CuO nanotubes has been successfully established, semiconductor ZnS and Nb_2O_5 nanotubes have been prepared by employing sacrificial template strategy based on liquid–solid reaction, and an in situ template method has been developed for the preparation of ZnO taper tubes through a chemical etching reaction. We have described the nanotube formation processes and illustrated the detailed key factors during their growth. The proposed mechanisms are presented for nanotube fabrication and the important pioneering studies are discussed on the rational design and fabrication of functional materials with tubular structures. It is the intention of this contribution to provide a brief account of these research activities.

Keywords Nanotubes · Chemical synthesis · Nanostructures · Inorganic materials

C. Yan · J. Liu · F. Liu · J. Wu · K. Gao · D. Xue (✉)
State Key Laboratory of Fine Chemicals, Department of Materials Science and Chemical Engineering, School of Chemical Engineering, Dalian University of Technology, Dalian 116012, China
e-mail: dfxue@chem.dlut.edu.cn

Introduction

Recently, considerable attention has been focused on micro- and nanostructured materials due to their unique properties and potential applications in many aspects [1–5], among which nanotubes have been attracting special interests since Iijima's identification of carbon nanotubes [5]. The tubular form is particularly attractive because it provides access to three different contact regions, inner and outer surfaces as well as both ends. However, for a long time the nanotube formation is generally limited to layered materials, through the bending of thin crystal flakes. Due to the weakness of interlayer interactions (van der Waals forces) and to the dangling bonds that can be eliminated by interlayer covalent bonds, nanotubes formation is very analogous to the case of carbon nanotubes based on a "rolling-up" mechanism [5]. A number of studies have been devoted to generating nanotubes from most kinds of materials [6–8], which clearly indicate that solid materials can be prepared as nanotubes by properly selecting proper preparation methods, for example, BN, V_2O_5, $NiCl_2$, TiO_2, and other materials with tubular structures [9–14].

Inorganic tubular structures become a symbol of the new and fast-developing research area due to their tremendous applications for over a decade. Inorganic nanotubes are less well studied, in part due to difficulties in well controlling their dimensions [15]. However, inorganic nanotubes still share many advantages of carbon nanotubes and can match increasing demand for various functions. Non-carbon materials [16], for example, titania nanotubes have been studied and show improved properties compared to colloidal or other forms of titania for applications in photocatalysis [17, 18], sensing [19], and photovoltaics [20, 21].

The past couple of decades have witnessed an exponential growth of activities in the synthesis of nanotubes,

driven by both excitement of understanding new science and the potential hope for applications and economic impacts. The numerous potential applications of inorganic nanotubes have been highlighted in a number of recent studies [17–21]. The present article reviews the classical methods and some recent contributions to the synthesis of nanotubes from inorganic materials that do not contain layered structure. We explicitly describe three different approaches for fabrication of tubular nanostructures, each approach is highlighted by at least one example.

Classical Preparation Methods

Rolling of Layered Materials for the Formation of Nanotubes

It is widely accepted that solid materials from layered precursors can be prepared as nanotubes by carefully controlling experimental conditions, based on a "rolling-up" mechanism. Two-dimensional layered compounds such as WS_2 [22], MoS_2 [23], and other structural analogues either roll up to form nanoscrolls or grow in rolled-up form, resulting in formation of single-wall or multi-wall nanotubes in gas atmosphere. The driving force lies in the built-in asymmetry of the unit cell along one zone axis and the thermal stress existing at high temperature, which initiates the scrolling of the layered sheets with reduced interlayer forces at the edges. Figure 1 is the model showing the process for the scrolling formation mechanism.

Similarly to the gas-action route, there have been significant research efforts devoted to nanotubes of layered or anisotropic crystal structured materials in solution, including $WO_3 \cdot H_2O$ [24], $Cu(OH)_2$ [25], $SrAl_2O_4$ [26], CeO_2 [27], and CeO_{2-x} [28]. The bending and roll-up of a thin layer to form tube is a thermally driven process. From a kinetic viewpoint, the rolling of layered structure may be initiated by a stress of either a structure or an electrical nature caused by the asymmetry of the layer. Though many nanotubes of layered or artificial lamellar structures have been successfully achieved, this strategy cannot be applied to non-layered materials.

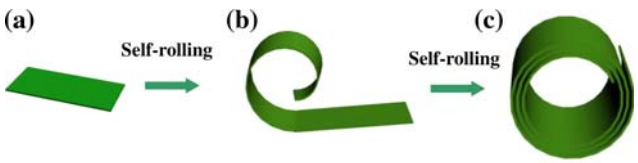

Fig. 1 Schematic illustration of nanotubes via rolling layered materials. **a** Formation of nanoplatelet. **b** An extension of reaction time results in the appearance of nanoscroll. **c** Nanotube formation through rolling nanoplatelet

Hard Templating Route for the Formation of Nanotubes

Templating approach is an important method to fabricate inorganic hollow tubes via high-temperature process [29–32]. The graphical representation of formation process of tubular structures is show in Fig. 2. Chemical vapor deposition (CVD), atomic layer deposition (ALD), and other vapor phase deposition techniques have been successfully employed to create conformal coating against existing templates. After the formation of core-sheath structures, the templates can be selectively removed by different chemical reactivities of core and shell components. Yang et al. employed the first "eptitaxial casting" process to synthesize single-crystalline GaN nanotubes [33]. As illustrated in Fig. 2, ZnO nanowires are used as template for the deposition of GaN thin films using metal-organic CVD. ZnO nanowires can be easily removed either in acidic solutions or via high-temperature reduction treatment. Because both ZnO and GaN have wurtzite crystal structure with similar lattice constants (<2% difference in the *a, b* parameters and <0.5% difference in the *c* parameter), this approach can provide single-crystalline GaN nanotubes by exploiting such an epitaxial relationship.

Similar to this approach, there is another versatile hard template strategy, which usually takes porous template such as anodic alumina oxide (AAO) and track-etched polymer membranes. During this process, the desired nanotube materials can be filled to the pores of porous template via precursor infiltration/wetting [34], electrochemical decoration [35], or ALD [36, 37], and followed by template removing, the desired materials nanotubes can be achieved. A typical procedure is shown in Fig. 3.

Although the template-based methods are regarded as a simple and very effective way for preparing nanotubes, this route requires the use of a base or acid medium or high temperature to remove templates, which increases the cost and risk of large-scale manufacture. Recently, a new

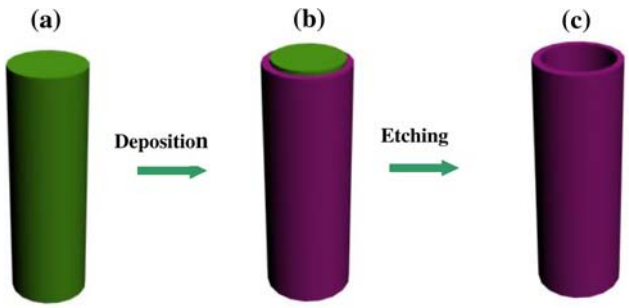

Fig. 2 Schematic illustration of nanotubes via nanorod or nanowire hard template. **a** Nanorod or nanowire template. **b** Core/shell structure intermediate. **c** Formation of nanotube through etching the inner core of intermediate

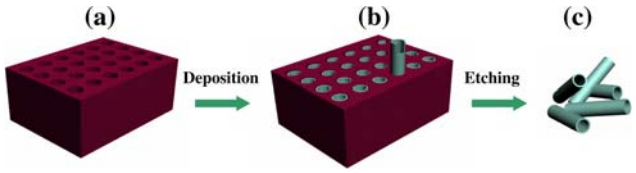

Fig. 3 Schematic illustration of nanotubes via a porous hard template such as AAO or track-etched polymer membranes

synthetic strategy is promoted, whereby nanorod or nanowire precursors are first generated in situ and act as the self-sacrificing template for growing nanotubes. The template can act not only as simply inert shape-defining molds but also as chemical reagents for the creation of nanotubes. For example, ultra-long single-crystal $ZnAl_2O_4$ spinel nanotubes were fabricated through a spinel-forming interfacial solid-state reaction of core-shell $ZnO–Al_2O_3$ nanowires involving the Kirkendall effect [38]. Single-crystal Cd_3P_2 and Zn_3P_2 nanotubes were synthesized by this chemical strategy [39]. This process involves the in situ formation of Zn and Cd metal cores, Cd_3P_2 and Zn_3P_2 shells, and finally the semiconductor nanotubes.

Soft Templating Route for the Formation of Nanotubes

Reverse micelles provide another example of the organized self-assembly of surfactants in solution and are most widely used as reaction media or templates for the synthesis of nanotubes. The hydrophilic head and hydrophobic tail of surfactants in a polar solvent self-assemble to give reverse micelles where the polar core contains the hydrophilic heads and the apolar shell the hydrophobic chains. The detailed formation processes of nanotubes are shown in Fig. 4.

Uniform goethite nanotubes with a parallelogram-shaped cross section have been fabricated via this synthetic procedure [40]. Hydrazine was added and induced the reaction with the Fe^{3+}–oleate complex. Subsequent crystallization resulted in the formation of 2 nm-sized spherical nanoparticles of iron oxide or related iron-containing compounds. Further aging induced the directional assembly of the 2 nm-sized nanoparticles onto the reverse micelle template, generating the nanotubes.

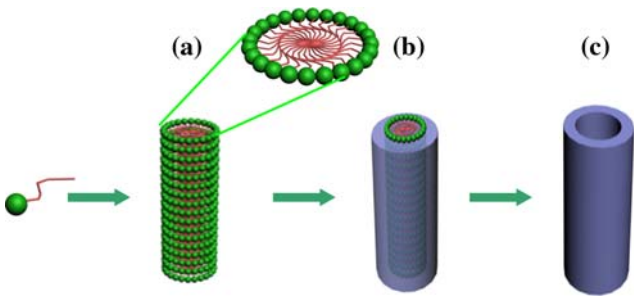

Fig. 4 Schematic illustration of nanotubes via templating against mesostructures self-assembled from surfactant molecules. **a** Formation of a cylindrical inverted micelle. **b** Formation of the desired material in the oil phase that the exterior surface of an inverted micelle serves as the physical template. **c** Removal of the surfactant molecules with an appropriate solvent (or by calcinations) to obtain an individual nanotube

Recently Developed Methods for the Synthesis of Nanotubes

Thermal Oxidation Method Based on Gas–solid Reaction

As a well-known transition metal oxide, copper oxide (CuO) has been extensively studied because of its applications in the field of lithium-ion batteries, catalysis, and superconductors [41]. We have proposed a general thermal oxidation method to synthesize porous CuO nanotubes based on a gas–solid reaction between CuSe nanowires and O_2 [41]. The current strategy is based on the combination of Kirkendall effect, volume loss, and gas release. Porous CuO nanotubes are used as example to demonstrate this general top–down chemical approach.

We first synthesized solid precursors of CuSe nanowires (Fig. 5a). Subsequently, these precursors were thermally oxidized in air at 700 °C. Simultaneously, core/shell-structured intermediates formed (Fig. 5b). Since the diffusion rate of the inner selenides is larger than that of atmospheric oxygen during the oxidation reaction stage, voids are thus generated, which eventually results in a tubular cavity (Fig. 5c). On heating CuSe precursor, a layer of CuO nanoparticles developed into a shell on the surface as the CuSe oxidized. Oxygen was still able to diffuse through this shell, the oxidation continued within during heating, CuSe diffused outwards faster than the CuO shell can diffuse inwards, leaving a hollow at the center of structure. This phenomenon is known as Kirkendall effect, and has been extensively exploited for producing hollow nanomaterials. The high porosity of the resulting shell structures was the result of the release of selenium dioxide from the objects, coupled with the volume loss on conversion from selenide to oxide. The holes that these processes created yielded porous shells. SEM images of the CuSe precursor and porous CuO nanotubes are shown in Fig. 5d and e, respectively. It is evident that the CuO nanotubes can be effectively prepared by employing thermal oxidation method based on a gas–solid reaction between CuSe nanowires and O_2.

The oxidation rate has an important effect on the morphology of final products. When the oxidation was carried out in a furnace at a previously maintained temperature of 700 °C, the non-equilibrium interdiffusion, volume loss,

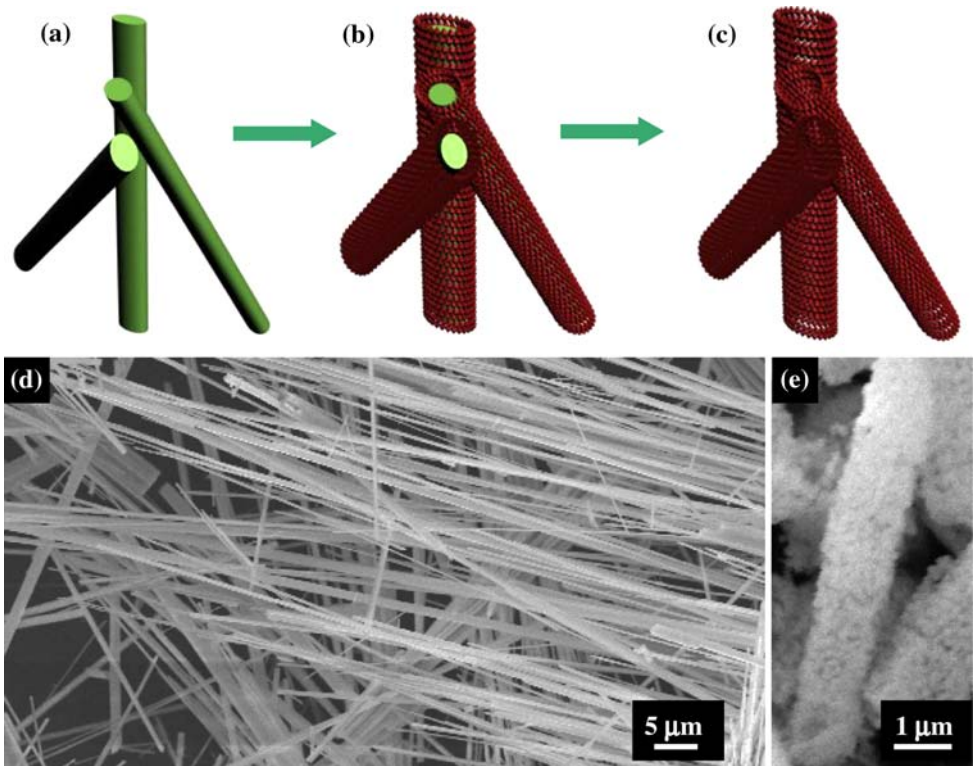

Fig. 5 Illustration of porous CuO nanotubes via a thermal oxidation process. **a** CuSe nanowires as the starting precursor. **b** Formation of CuO at the shell of CuSe in the thermal oxidation process. **c** Continual growth of CuO from CuSe, which involves a non-equilibrium interdiffusion, volume loss, and release of internally born gas, and eventual formation of porous CuO nanotubes. **d** SEM image of CuSe nanowires precursor. **e** SEM image of porous CuO nanotube using as-prepared CuSe nanowire as the precursor

and gas release strongly accelerated, and the tubular structure then collapsed. The obtained CuO nanotubes with a porous shell might be more attractive than closed hollow structures in some aspects such as catalysis, because of the dense distribution of pores in their walls. More importantly, our thermal oxidation method is quite versatile and can be extended to other transition metal chalcogenides.

Sacrificial Template Strategy Based on Liquid–Solid Reaction

Metal Sulfides

As a very important direct wide-band-gap semiconductor with the highest band gap of 3.6 eV among all II–VI compounds, ZnS has received much attention due to its excellent properties and is extensively used as displays, sensors, and lasers [42, 43]. Recently, nanoscale metal sulfides are assuming great importance in both theory and practice, owning to their novel properties as a consequence of a large number of surface atoms and the three-dimensional confinement of electrons [44]. These unique properties lead to appearance of many new application areas such as solar cells, photodetectors, light-emitting diodes, and laser communication.

As for the sacrificial template strategy based on liquid–solid reaction, a nanotube was formed by creating at least one sheath layer around a nanowire template. The nanowire template functions as a sacrificial core which was later removed to establish the central opening through the nanotube. Once the sacrificial core was removed, the nanotube can be used in any conventional manner. Figure 6 illustrates the general steps in what we refer to as a "template method" approach. ZnS nanotubes were formed in a sulfuration process and the nanowire cores were removed in an etching process [43]. The nanotube cores (templates) were created from ZnO nanowires. The process comprises sulfuration of the ZnO nanowire arrays (Fig. 6a), which results in arrays of thin ZnO nanowires sheathed by a thick layer of ZnS. Figure 6b shows a schematic drawing of the ZnO/ZnS nanocables on the zinc foil substrate, with ZnO as the core and ZnS as the shell. It can be clearly demonstrated that ZnO nanorods were wrapped with a thin layer of ZnS. This sulfide nanowire array was then selectively etched, for example, with KOH or NaOH to remove the ZnO nanowire cores, leaving an array of ordered ZnS nanotubes (Fig. 6c) with controllable inner diameters. The inner diameters were controlled by the initial diameters of the ZnO nanowires and the following sulfuration process. It is contemplated that, with further refinements of the sulfuration and etching processes, nanotubes with various diameters can be produced in this manner.

An evolution in particle shape from ZnO nanorod to ZnS nanotube array is due to the solubility difference between ZnO and ZnS and to the assistance of thioglycolic acid.

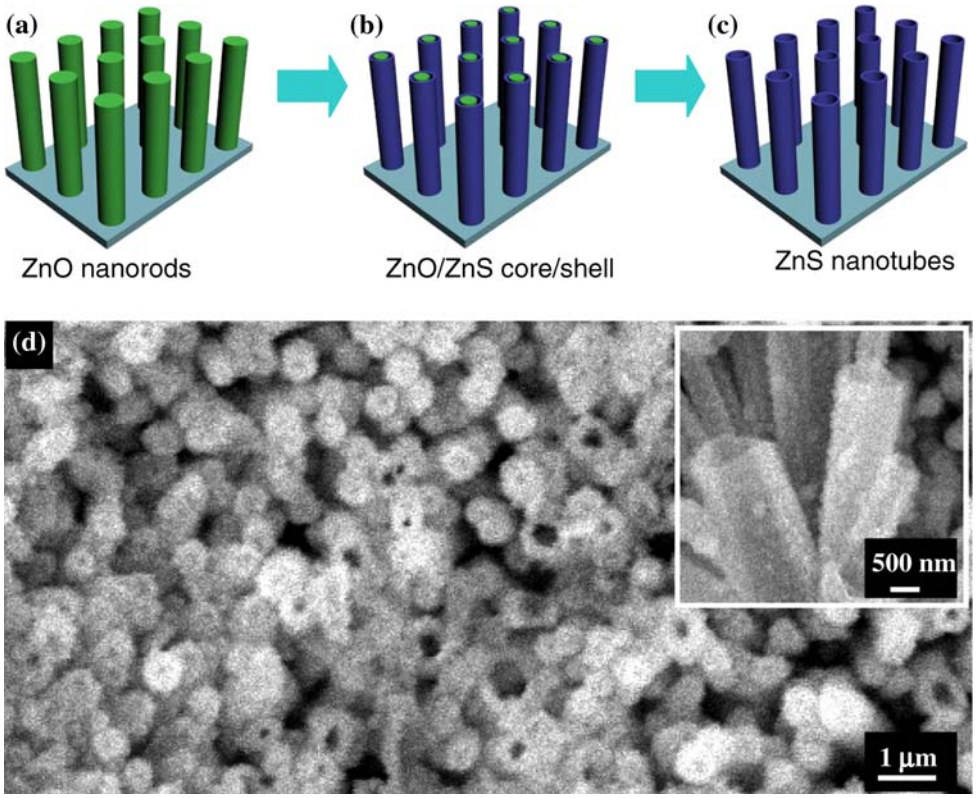

Fig. 6 Illustration of ZnS nanotubes via a sacrificial strategy. **a** ZnO nanorods as the starting precursors. **b** Formation of ZnS at the shell of ZnO through sulfuration reaction. **c** Etching ZnO cores to form ZnS nanotubes. **d** SEM image of ZnS nanotubes using as-prepared ZnO nanorods as the precursor

ZnO nanorod arrays were used as a template for the fabrication of ZnO/ZnS nanocables by sulfurization of ZnO after a thioglycolic acid-assisted reaction. When ZnO nanorod arrays were introduced into $HSCH_2COOH$ solution, $ZnHS^+$ complex could be formed between the lone pair electrons of sulfur atom of $HSCH_2COOH$ molecule and the vacant *d* orbital of the Zn^{2+} ions, which results in an increase in the activity of Zn^{2+} ions on ZnO nanorods, and then ZnS nucleates and grows by dissolution of ZnO nanorods. After reaction, ZnO/ZnS nanocables can be obtained. Since ZnO has an amphoteric characteristic, KOH treatment of ZnO/ZnS nanocables leads to the dissolution of ZnO cores, and thus ZnS nanotube arrays can be successfully obtained. The well-aligned ZnS nanotube arrays were observed on the surface of zinc foil, as shown in Fig. 6d. It can be seen that ZnS tubes have open ends with a uniform pore size.

Metal Oxide Nanotubes

Oxide nanotubes of several transition metals and other metals have been synthesized employing different methodologies. As one of the group V–B oxides, niobium oxide (Nb_2O_5) is an important *n*-type semiconductor with a wide band gap of about 3.4 eV, and has found important applications in solar cells, sensors, advanced catalysts, and electrochromic devices [45].

It is a novel sacrificial template route to prepare Nb_2O_5 nanotube by employing pseudo hexagonal Nb_2O_5 as template to monoclinic products. Monoclinic Nb_2O_5 with tunable diameter was fabricated through a phase transformation process between pseudo hexagonal and monoclinic Nb_2O_5 nanotube, which involves a non-equilibrium interdiffusion process accompanied by the void generation in solution reaction system. A key parameter for achieving nanotube growth is the energy difference between the pseudo hexagonal and monoclinic Nb_2O_5 nanostructures, which determines the phase transformation.

With pseudo hexagonal Nb_2O_5 (TT-Nb_2O_5) nanorod arrays serving as template (Fig. 7a), Nb_2O_5 core-shell arrays (Fig. 7b) could be produced. In this process monoclinic Nb_2O_5 (H-Nb_2O_5) was obtained from TT-Nb_2O_5 and core/shell structures consisting of pseudo hexagonal cores and monoclinic shell thin layer were formed. This thin layer acts as an interface that separates the inner core from the outside shell. At the shell the nuclei grow through consuming core materials, with prolonging growth time, the core and shell start to get separated by a clear gap. Small voids can be observed between TT-Nb_2O_5 core and H-Nb_2O_5 shell, indicating condensation of vacancies at the boundary. Further phase transformation and void formation depend on the diffusion or migration of TT-Nb_2O_5 (either in the form of niobium and oxygen ions, or in the form of niobium–oxygen cluster) through the formed H-Nb_2O_5

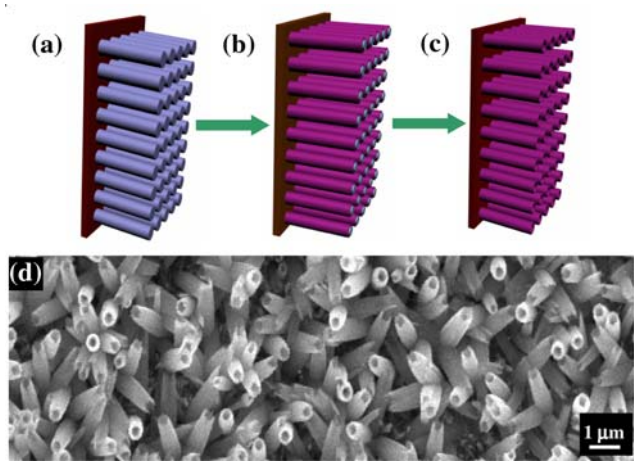

Fig. 7 Illustration of monoclinic Nb_2O_5 nanotube arrays via a sacrificial template of TT-Nb_2O_5. **a** TT-Nb_2O_5 nanorod array as the starting precursor. **b** Core/shell-structured Nb_2O_5. **c** H-Nb_2O_5 nanotube arrays. **d** SEM image of monoclinic Nb_2O_5 nanotube array

shell interfaces. The driving force for phase transformation is the tendency of the system to reduce its interfacial energy. Moreover, changes in the reaction energy and the height of reaction barriers inevitably accompany the well-known increase in diffusion rate. The increased interface diffusion of atoms during the phase transformation process enhances the void formation. Therefore, as the reaction proceeds in time, more TT-Nb_2O_5 core materials diffuse out to the shell, and the accompanying transport of vacancies leads to the growth and merging of voids. All TT-Nb_2O_5 nanorods can be completely converted into hollow H-Nb_2O_5 nanotubes as the reaction proceeds to 48 h (Fig. 7c). SEM image of H-Nb_2O_5 nanotubes clearly indicates that these nanotubes have completely hollow structures without filling or blockage (Fig. 7d). The nanotube has open ends with a uniform pore size in the range of 200–500 nm and wall thickness in the range of 50–100 nm. The size of H-Nb_2O_5 nanotubes can be tunable by adjusting the diameter of TT-Nb_2O_5 nanorods.

In situ Template Method Based on Chemical Etching Reaction

Currently, the template-directed synthesis of functional materials is arousing increasing interest due to its unique advantages in the control over shape, size, and crystal growth [2, 43, 46]. It represents a straightforward and efficient route towards hollow structures. However, these reported template strategies often suffer from the great difficulty to separate hollow structures from template, which is still a big challenge for the synthesis of hollow structures. We believe that direct methods in which synthesis and template elimination are coupled in situ to produce hollow structures have great applications, due to the fact that the difficulty of removing template from the reaction system can be effectively avoided. ZnO, a well-known direct-bandgap semiconductor, represents one of the most important materials of the wurtzite family, with many remarkable applications in electronics, photoelectronics, and sensors [47–49].

The hexagonal wurtzite structure ZnO can be simply described as a number of alternating planes composed of tetrahedrally coordinated O^{2-} and Zn^{2+} ions, stacked alternately along the *c*-axis. Considering the atom arrangement forms of the specific planes, the (001) face of ZnO crystal contains Zn atom only, whereas (00-1) face consists of oxygen atom. The positively charged ZnO (001)-Zn surface is chemically active, and the negatively charged (00-1)-O surface is inert. Therefore, the selectively etching ZnO taper appears to take place preferentially at the (001) face, which is a typical phenomenon for wurtzite-structured materials well interpreted by chemical bonding theory [3]. Herein, we have developed an in situ template strategy for the synthesis of ZnO tubes through chemical etching reaction, which avoids the multiple steps that are currently used in the preparation of other hollow materials [47]. The chemical etching in situ formed ZnO template is related to its intrinsic symmetry of the corresponding lattice and chemical activities.

Figure 8a is a typical SEM image of the synthesized ZnO hollow structures with tube-like morphology on the zinc foil. The ZnO taper template can be formed at the early reaction stage, which can be effectively acted as the in situ template for the subsequent generation of hollow ZnO tubes. Template of truncated ZnO tapers was directly etched onto the areas selected from the six corners of top

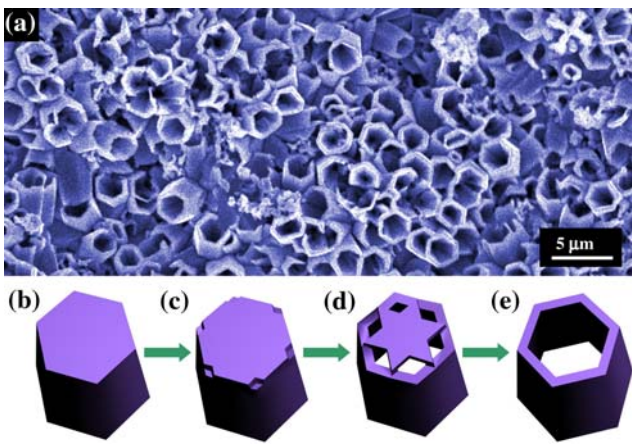

Fig. 8 Illustration of ZnO tubes via a chemical etching process. **a** SEM image of ZnO tube through an in situ template route based on a chemical etching reaction. Formation mechanism of in situ template route: **b** formation of truncated ZnO template. **c** Six pits observed at the six corners of the top surface of an truncated ZnO taper after etching. **d** Further etching of the truncated taper. **e** Formation of ZnO tube by dissolving ZnO core

surface by dissolving ZnO core in the acetic acid solution. Schematic drawing of Fig. 8 summarizes all major steps involved in the chemical etching reaction process, which are consistent with the corner-etched structure of the tubular ZnO. The whole etching process can be divided into four reaction stages, which clearly reveal the selective etching mechanism involved in the formation of hollow ZnO tubes. At the initial stage, truncated ZnO taper is obtained (Fig. 8b), which was used as the in situ template for the synthesis of hollow ZnO tubes. Subsequently, the etching starts on the hexagonal top surface of the already formed template (truncated tapers) by acetic acid, when the reaction was proceeded, six pits were thus observed at the six corners of hexagonal top surfaces of an individual truncated taper (Fig. 8c). When the reaction time was extended, six gradual widening holes located at the hexagonal top surface of an individual truncated taper can be generated (Fig. 8d). Tubular structures (Fig. 8e) were formed after a complete etching of the core of truncated taper as the etching reaction proceeds to a longer reaction time.

Conclusions

The inorganic nanotubes possess several characteristics that are beneficial for their applications in optoelectronics and catalysis. In particular, the ability to synthesize and control the inner diameter of nanotubes makes the nanotube-based device/system a unique tool for further applications. This article summarizes recent progresses on the synthesis of inorganic nanotubes. New synthetic strategies for the tube formation in nanoscale have been developed. Three different approaches to the production of high-quality semiconductor nanotubes have been demonstrated. A thermal oxidation route by employing gas–solid reaction to porous CuO nanotubes, a sacrificial template strategy for the synthesis of ZnS and Nb_2O_5 nanotubes based on liquid–solid reaction, and an in situ template route to ZnO taper tubes through a chemical etching reaction have been successfully developed. Combined together, these approaches have greatly expanded the scope of inorganic materials that can be processed as nanotubes with uniform and controllable dimensions. We believe that these techniques can be readily extended to produce more complex nanostructures with hollow interiors and cover a broader range of materials than those presented in this article by incorporating more reactions and thus more solid materials into the synthetic process. The scientific and technical potential of these novel nanotube structures are certainly bright and there are great research opportunities that will be explored by many chemists, physicists, and material scientists around this general area.

Acknowledgments The authors gratefully acknowledge the financial support of NCET-05-0278, NSFC #20471012, and FANEDD #200322.

References

1. S.A. Corr, Y.P. Rakovich, Y.K. Gunko, Nanoscale Res. Lett. **3**, 87 (2008). doi:10.1007/s11671-008-9122-8
2. C. Yan, D. Xue, J. Phys. Chem. B **110**, 7102 (2006). doi:10.1021/jp057382l
3. X. Yan, D. Xu, D. Xue, Acta Mater. **55**, 5747 (2007). doi:10.1016/j.actamat.2007.06.023
4. C. Yan, D. Xue, J. Phys. Chem. B **110**, 1581 (2006). doi:10.1021/jp056373+
5. S. Iijima, Nature **354**, 56 (1991). doi:10.1038/354056a0
6. Y. Xiong, B. Mayers, Y. Xia, Chem Commun (Camb) 5013. (2005). doi:10.1039/b509946c
7. I. Avramov, Nanoscale Res. Lett. **2**, 235 (2007). doi:10.1007/s11671-007-9054-8
8. Y. Piao, J. Kim, H.B. Na, D. Kim, J.S. Baek, M.K. Ko, J.H. Lee, M. Shokouhimehr, T. Hyeon, Nat. Mater. **7**, 242 (2008). doi:10.1038/nmat2118
9. N.G. Chopra, R.J. Luyken, K. Cherrey, V.H. Crespi, M.L. Cohen, S.G. Louie, A. Zettl, Science **269**, 966 (1995). doi:10.1126/science.269.5226.966
10. M.E. Spahr, P. Bitterli, R. Nesper, M. Muller, F. Krumeich, H.U. Nissen, Angew. Chem. Int. Ed. **37**, 1263 (1998). doi:10.1002/(SICI)1521-3773(19980518)37:9<1263::AID-ANIE1263>3.0.CO;2-R
11. Y.R. Hacohen, E. Grunbaum, R. Tenne, J. Sloan, J.L. Hutchison, Nature **395**, 336 (1998). doi:10.1038/26380
12. Y. Li, J. Wang, Z. Deng, Y. Wu, X. Sun, D. Yu, P. Yang, J. Am. Chem. Soc. **123**, 9904 (2001). doi:10.1021/ja016435j
13. V. Vega, V.M. Prida, M. Hernandez, E. Manova, P. Aranda, E. Ruiz-Hitzky, M. Vazquez, Nanoscale Res. Lett. **2**, 355 (2007). doi:10.1007/s11671-007-9073-5
14. F. Liu, C.T. Sun, C. Yan, D. Xue, J. Mater. Sci. Technol. **24**, 641 (2008). doi:10.1179/174328408X270347
15. M.S. Sander, M.J. Cote, W. Gu, B.M. Kile, C.P. Tripp, Adv. Mater. **16**, 2052 (2004). doi:10.1002/adma.200400446
16. G.R. Patzke, F. Krumeich, R. Nesper, Angew. Chem. Int. Ed. **41**, 2446 (2002). doi:10.1002/1521-3773(20020715)41:14<2446::AID-ANIE2446>3.0.CO;2-K
17. M. Adachi, Y. Murata, M. Harada, S. Yoshikawa, Chem. Lett. **29**, 942 (2000). doi:10.1246/cl.2000.942
18. S.Z. Chu, S. Inoue, K. Wada, D. Li, H. Haneda, S. Awatsu, J. Phys. Chem. B **107**, 6586 (2003). doi:10.1021/jp0349684
19. O.K. Varghese, D.W. Gong, M. Paulose, K.G. One, E.C. Dickey, C.A. Grimes, Adv. Mater. **15**, 624 (2003). doi:10.1002/adma.200304586
20. S. Uchida, R. Chiba, M. Tomiha, N. Masaki, M. Shirai, Electrochemistry **70**, 418 (2002)
21. M. Adachi, Y. Murata, I. Okada, S. Yoshikawa, J. Electrochem. Soc. **150**, G488 (2003). doi:10.1149/1.1589763
22. R. Tenne, L. Margulis, M. Genut, G. Hodes, Nature **360**, 444 (1992). doi:10.1038/360444a0
23. Y. Feldman, E. Wasserman, D.J. Srolovitz, R. Tenne, Science **267**, 222 (1995). doi:10.1126/science.267.5195.222
24. Z.X. Wang, S.X. Zhou, L.M. Wu, Adv. Funct. Mater. **17**, 1790 (2007). doi:10.1002/adfm.200601195
25. W.X. Zhang, X.G. Wen, S.H. Yang, Y. Berta, Z.L. Wang, Adv. Mater. **15**, 822 (2003). doi:10.1002/adma.200304840
26. C.H. Ye, Y. Bando, G.Z. Shen, D. Golberg, Angew. Chem. Int. Ed. **45**, 4922 (2006). doi:10.1002/anie.200601320

27. C.C. Tang, Y. Bando, B.D. Liu, D. Geolberg, Adv. Mater. **17**, 3005 (2005). doi:10.1002/adma.200501557
28. W.Q. Han, L.J. Wu, Y.M. Zhu, J. Am. Chem. Soc. **127**, 12814 (2005). doi:10.1021/ja054533p
29. Z. Wang, M. Brust, Nanoscale Res. Lett. **2**, 34 (2007). doi:10.1007/s11671-006-9026-4
30. Z. Liu, D. Zhang, S. Han, C. Li, B. Lei, W. Lu, J. Fang, C. Zhou, J. Am. Chem. Soc. **127**, 6 (2005). doi:10.1021/ja0445239
31. L. Zhao, M. Yosef, E. Pippel, H. Hofmeister, M. Steinhart, U. Dosele, S. Schlecht, Angew. Chem. Int. Ed. **45**, 8042 (2006). doi:10.1002/anie.200602093
32. X.W. Lou, D. Deng, J.Y. Lee, J. Feng, L.A. Archer, Adv. Mater. **20**, 258 (2008). doi:10.1002/adma.200702412
33. J. Goldberger, R. He, Y. Zhang, S. Lee, H. Yan, H.J. Choi, P. Yang, Nature **422**, 599 (2003). doi:10.1038/nature01551
34. L. Zhao, T.Z. Lu, M. Zacharias, J. Yu, J. Shen, H. Hofmeister, M. Steinhart, U. Gosele, Adv. Mater. **18**, 363 (2006). doi:10.1002/adma.200501974
35. W. Lee, R. Scholz, K. Nielsch, U. Gosele, Angew. Chem. Int. Ed. **44**, 6050 (2005). doi:10.1002/anie.200501341
36. J. Bachmann, J. Jing, M. Knez, S. Barth, H. Shen, S. Mathur, U. Gosele, K. Nielsch, J. Am. Chem. Soc. **129**, 9554 (2007). doi:10.1021/ja072465w
37. H. Shin, D.K. Jeong, J. Lee, M.M. Sung, J. Kim, Adv. Mater. **16**, 1197 (2004). doi:10.1002/adma.200306296
38. H.J. Fan, M. Knez, R. Scholz, K. Nielsch, E. Pippel, D. Hesse, M. Zacharias, U. Gosele, Nat. Mater. **5**, 627 (2006). doi:10.1038/nmat1673
39. G. Shen, Y. Bando, C. Ye, X. Yuan, T. Sekiguchi, D. Golberg, Angew. Chem. Int. Ed. **45**, 7568 (2006). doi:10.1002/anie.200602636
40. T. Yu, J. Park, J. Moon, K. An, Y.Z. Piao, T. Hyeon, J. Am. Chem. Soc. **129**, 14558 (2007). doi:10.1021/ja076176j
41. J. Liu, D. Xue, Adv. Mater. **20**, 2622 (2008). doi:10.1002/adma.200800208
42. G. Morello, M. Anni, P.D. Cozzoli, L. Manna, R. Cingolani, M. De Giorgi, Nanoscale Res. Lett. **2**, 512 (2007). doi:10.1007/s11671-007-9096-y
43. C. Yan, D. Xue, J. Phys. Chem. B **110**, 11076 (2006). doi:10.1021/jp060357a
44. A. Henglein, Chem. Rev. **89**, 1861 (1989). doi:10.1021/cr00098a010
45. C. Yan, D. Xue, Adv. Mater. **20**, 1055 (2008). doi:10.1002/adma.200701752
46. C. Yan, D. Xue, Funct. Mater. Lett. **1**, 37 (2008). doi:10.1142/S1793604708000083
47. C. Yan, D. Xue, Electrochem. Commun. **9**, 1247 (2007). doi:10.1016/j.elecom.2007.01.029
48. D.K. Bhat, Nanoscale Res. Lett. **3**, 31 (2008). doi:10.1007/s11671-007-9110-4
49. T. Dedova, O. Volobujeva, J. Klauson, A. Mere, M. Krunks, Nanoscale Res. Lett. **2**, 391 (2007). doi:10.1007/s11671-007-9072-6